Near-source energy released of 2003 Bam earthquake using slip-weakening law

Mohammad Reza Ghayamghamian & Mohammad Sasani
International institute of earthquake engineering and seismology, Tehran, Iran

SUMMARY:
Dynamic source models are needed to accomplish the simulation and prediction of earthquake ground motions. Propagation of earthquake ruptures along the fault plane is accompanied by the dynamic fault weakening. This weakening is represented by the slip-weakening law, which defines the traction decreasing from an upper yield stress to the residual stress as slip increases. In this paper, an attempt is made to estimate dynamic source parameters of 2003 Bam earthquake based on source parameters inverted from kinematic model. To this end, Fukuyama's new energy balance relation under linear slip-weakening model together with the identified slip model for Bam earthquake by first author is used. Then, the dynamic source parameters such as slip-weakening distance, stress drop and strength excess are calculated. Furthermore, the released energy in the form of fracture and radiated energies and their distribution on the fault are estimated and discussed. Finally, the radiation efficiency from the partitioning of energy given by the slip-weakening model is estimated and compared with some crustal earthquakes.

Keywords: near-source energy, slip-weakening law, fracture energy, Bam earthquake

1. INTRODUCTION

One of the most important source parameters is the energy released of an earthquake, which affects both fault dynamic characteristics and type of ruptures. During an earthquake, potential energy (elastic strain energy) released in three ways: fracture energy (E_F), frictional heat or thermal energy (E_H) and the energy radiated as seismic waves (E_r) (Tinti, Spudich and Cocco 2005). Several models such as seismological (e.g. Rice et al. 2005; Tinti et al. 2005) and geological (Chester et al., 2005; Wilson et al., 2005) measurements of energies absorbed on faults have been proposed to estimate energy of an earthquake. These models used to describe a physical process of fault rupture with released energy. In this study, Linear Slip-Weakening model (LSW), proposed by Ida (1972), is used to evaluate the near-source energy released of the 2003 Bam earthquake.

On the 26th December 2003 an earthquake with M_W=6.5 shook a large area of the Kerman Province in south-east of Iran causing more than 26000 fatalities. The hypocenter of the Bam earthquake was located at 29.01◦N, 58.26◦E, at a depth of 10 km in the southwest of Bam city. More than 26000 people were killed, 30000 injured, up to 75000 left homeless, and 85 percent of the housing and infrastructure were destroyed due to this earthquake (Ghayamghamian and Hisada, 2007). Several rupture models have been proposed for Bam earthquake (2003). Nakamura et al. (2005) explained a fault plane with an N–S alignment, which was located 5 km west of the old Bam fault. Talebian et al. (2004) suggested a source model by adopting the mechanism from teleseismic observations. It consisted of a main strike-slip fault, and an additional pure trust fault. Wang et al. (2004) proposed a fault model consisting of three straight segments based on Envisat Asar data. The southern segment is about 13 km, the northern one is about 6 km and the middle segment is disappeared below the city area of Bam and is considered to be a 5 km segment connecting the southern and northern segments. The total length of the ruptured fault is about 24 km consisting of these three segments. They concluded that more than 80 percent of the seismic moment was released from the southern fault segment of 13–14 km long. The southern segment corresponds about to the strike-slip fault suggested by Nakamura et al. (2005). Ghayamghamian and Hisada (2007) used Wang model to simulate strong ground motion in Bam station located just 700 m from causative fault. They found that the fault model including the southern and middle segments could fully explains the observed ground motion in Bam station. Their slip model of Bam fault consists of two asperities that are located in front and bellow the hypocenter for the southern segment, and one big shallow asperity for the middle segment. The asperities are embedded in a background slip that corresponds to the entire fault rupture area. In this paper, their slip model is used to estimate dynamic source parameters and the energy released of Bam earthquake.

2. SLIP-WEAKENING LAW

In the standard model of stick-slip mechanism, it is assumed that sliding begins when the ratio of shear to normal stress on contact surfaces reaches to the value of static friction coefficient. Then, sliding occurs and the coefficient of friction decreases and reaches to the dynamic friction coefficient (Scholz 1998; Xing, Mora et al. 2006). A general mechanism of stick-slip process has been explained by Reid's elastic rebound theory. This process begins with stress accumulation in which stresses of fault increase until overcoming to fault strength. After that, stresses release and slip phase occurs (Senatorski 2002).

Here, linear slip-weakening law is adopted to estimate the near-source released and fracture energies of Bam causative fault. There are several reasons for this selection. First, this law has strong support in laboratory experiments, and can be used for both the case of frictional slip failure on pre-existing faults and shear failure of intact rocks. Second, kinematic model of earthquakes give some support to the slip-weakening constitutive formulation. Third, a slip-weakening constitutive formulation is applicable for theoretical treatment of both the fracture and frictional slip phenomena, and has interpretation in terms of energy change of the system (Senatorski 2002).
According to slip-weakening law, an earthquake occurs when a fault weakens during the early stage of its slip at a faster rate than the release of tectonic stress driving the fault motion. This slip weakening occurs over a critical distance, D_c (Wibberley and Shimamoto, 2005). Like other rock friction laws, slip-weakening is a laboratory derived friction law and it has three parameters, which are estimated based on experimental results. The linear slip-weakening can be given as:

$$\begin{aligned} \mu(x) &= \mu_s - \frac{x}{D_c}(\mu_s - \mu_d) && 0 \le x \le D_c \\ \mu(x) &= \mu_d && D_c < x \end{aligned} \qquad (2.1)$$

Where μ_s is static coefficient of friction, μ_d is dynamic coefficient of friction, D_c is slip-weakening distance; x is displacement, $\mu(x)$ is coefficient of friction corresponding to displacement. Understanding the magnitude of D_c in nature is severely limited. Conventional friction experiments, typically conducted at slow slip rates and small displacements, have obtained D_c values that are in orders of magnitude lower than the values estimated from seismological data modelling for natural earthquakes. In the following sections, the slip-weakening parameters are discussed.

2.1. Slip-Weakening Distance

The slip-weakening distance (D_c) is the most important parameter of dynamic rupture of an earthquake, which controls the nucleation process of earthquake (Fukuyama, Mikumo and Olsen 2003). Several methods are proposed to estimate slip-weakening distance such as laboratory experiments, numerical calculations and theoretical approaches. Mikumo et al. (2003) used slip velocity functions on the fault to estimate D_c. In their method, it is assumed that the time of peak slip velocity and stress breakdown time are similar and therefore, D_c is the slip at the time of peak slip velocity (Mikumo, et al. 2003). They suggested two limits for the ratio of slip-weakening distance to final slip (D_c/D_{tot}) as:

$0.27 < D_c/D_{tot} < 0.56$ (2.2)

Tinti et al. (2009) performed a series of numerical tests to understand the dependence of the slip-weakening distance (D_c) on the final slip (D_{tot}) during the propagation of a dynamic rupture. They suggest histograms for the ratio of D_c/D_{tot} that shows larger frequency for the ratio of 0.4 and 0.5 (Tinti, et al. 2009).

2.2. Stress Changes

There are two parameters in relation to stress changes based on slip-weakening law: stress drop and strength excess. Furthermore, two types of stress drop are defined as (1) static stress drop that is the difference between the initial shear stress and the final shear stress and (2) dynamic stress drop that is the difference between the initial shear stress and the shear stress during sliding (Fig. 2.1).

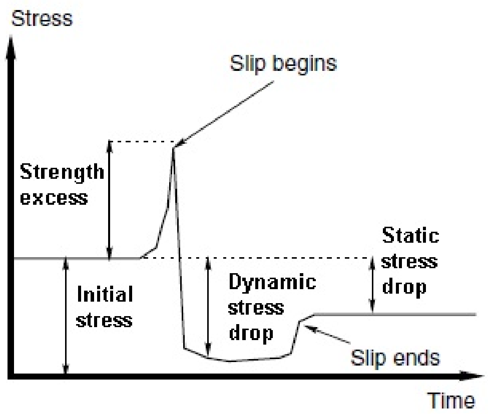

Figure 2.1. Variation of shear stress in a fix location on fault as a function of time

Stress drop which is used for calculation of near-source energy is dynamic stress drop. For estimating the dynamic stress drop, static stress drop should be first calculated. For strike–slip mechanism on a shallow, rectangular fault of length L and width W (L >> W), Knopoff (1958) obtained:

$$\Delta\sigma = \frac{2\mu\overline{D}}{\pi W} \tag{2.3}$$

where $\Delta\sigma$ is static stress drop, μ is shear modulus of rock, $\overline{D}$ is average slip and W is width of the fault (Knopoff 1958). Shear modulus is calculated using following equation:

$$\mu = \rho V_s^2 \tag{2.4}$$

where ρ is density and V_s is shear wave velocity. Mai et al. (2006) proposed a relation between dynamic stress drop and static stress drop as:

$$\Delta\sigma_d = 0.048 + 0.948\Delta\sigma \tag{2.5}$$

where $\Delta\sigma_d$ is dynamic stress drop.

According to slip-weakening model, before the slip phase, stress accumulates behind the crack tip until reaching to the value of yield stress. This increase in stress is called strength excess, which here assumed to be $1.6\,\Delta\sigma_d$ (Andrews 1976). This is because the resultant rupture velocity does not exceed the shear wave velocity and the rupture propagates stably when the strength excess is about 1.6 times the dynamic stress drop.

3. ENERGY BUDGET IN EARTHQUAKE

During an earthquake, stress on the fault planes changes rapidly and causes the potential release energy of fault (Rivera and Kanamori 2005). As mentioned above, the total energy release in three ways as schematically shown in Fig. 3.1. Beneath the frictional level of shear stress, the potential energy dissipates as frictional heat or thermal energy throughout the slip phase but above this level of shear stress, the potential energy is released in the forms of fracture energy and radiated energy.

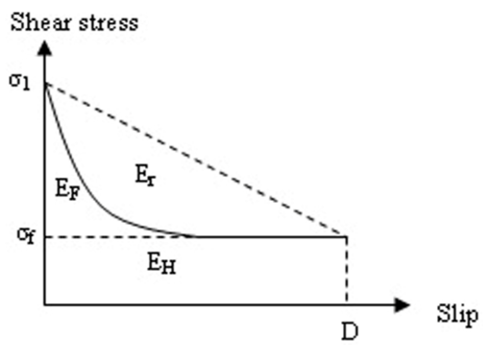

Figure 3.1. Simple representation of energy budget for earthquake

Fukuyama (2005) proposed a new concept for energy released close to the fault surfaces which can be expressed as:

$$E_r' = \int_{\Sigma}\left[\left(\sigma_{ij}^0 - \sigma_{ij}^1\right)a_i^1 n_j + \int_{t_0}^{t_m}\left({}^{d\sigma_{ij}}\!/_{dt}\right)a_i n_j\,dt\right]dS \tag{3.1}$$

where σ_{ij} is stress component, a_i is the displacement between fault surface, n_j is the unit vector normal to the surface, Σ is fault surface, t_0 and t_m are initial time and time of termination of rupture, respectively and superscript 0 and 1 are corresponding to t_0 and t_m, respectively (Fukuyama 2005). Linear slip-weakening law is used for dynamic rupture in which initial shear stress (σ_0) increase up to the yield stress (σ_y). After that, shear stress decrease linearly with slip and reaches to dynamic friction stress (σ_f). Using these parameters in Eqn. 2.1 will result in Eqn. 5.1 as:

$$E_r' = \int_{\Sigma}(\sigma_0 - \sigma_f)D\,dS - \frac{1}{2}\int_{\Sigma}(\sigma_y - \sigma_f)D_c\,dS \tag{3.2}$$

The first term in the right hand side of Eqn. 5.1 corresponds to twice the strain energy change (ΔW) due to slip under stress change and the second term is the fracture energy (Mikumo and Fukuyama 2006). Thus, the near-source energy and fracture energy for each segment of fault plane could be estimated as:

$$E'_{ri} = \left[\Delta\sigma D - \frac{1}{2}(\Delta\sigma + \Delta\sigma_e) D_c \right] A_i$$
$$E_{Fi} = \left[\frac{1}{2}(\Delta\sigma + \Delta\sigma_e) D_c \right] A_i \qquad (3.3)$$

where $\Delta\sigma$ is dynamic stress drop, $\Delta\sigma_e$ is strength excess and A_i is the area of each segment. Then, the total near-source energy and fracture energy are estimated by Eqn. 5.3:

$$E'_r = \sum E'_{ri}$$
$$E_F = \sum E_{Fi} \qquad (3.4)$$

4. ESTIMATION OF DYNAMIC PARAMETERS FOR 2003 BAM EARTHQUAKE

In this section, all parameters that are required for estimating the energy released of Bam earthquake are discussed. The base of all calculations is the distribution of final slip on the fault plane, which is estimated using kinematic modelling by Ghayamghamian and Hisada (2007). In the following, after giving a brief explanation of Bam slip model, the procedure that lead to estimate dynamic source parameters of Bam earthquake will be described.

4.1. Slip Model of Bam Fault

The slip model of 2003 Bam earthquake is determined by several researchers (Wang et al., 2004; Funning et al., 2005 and Ghayamghamian and Hisada 2007). The latest research was provided by Ghayamghamian and Hisada (2007) based on kinematic inversion of near-fault ground motions. This model, which fully described the recorded near-fault and near-field ground motions, was adopted here for the analysis. Their model is shown in Fig. 4.1 where the main asperity located near the surface with maximum slip of about 2 m. This model include two fault segments (southern and middle segments), which more than 80 per cent of the seismic moment was released from the southern segment (Ghayamghamian and Hisada 2007). Consequently, the slip model of southern segment is used to evaluate dynamic source parameters and released energy of Bam earthquake.

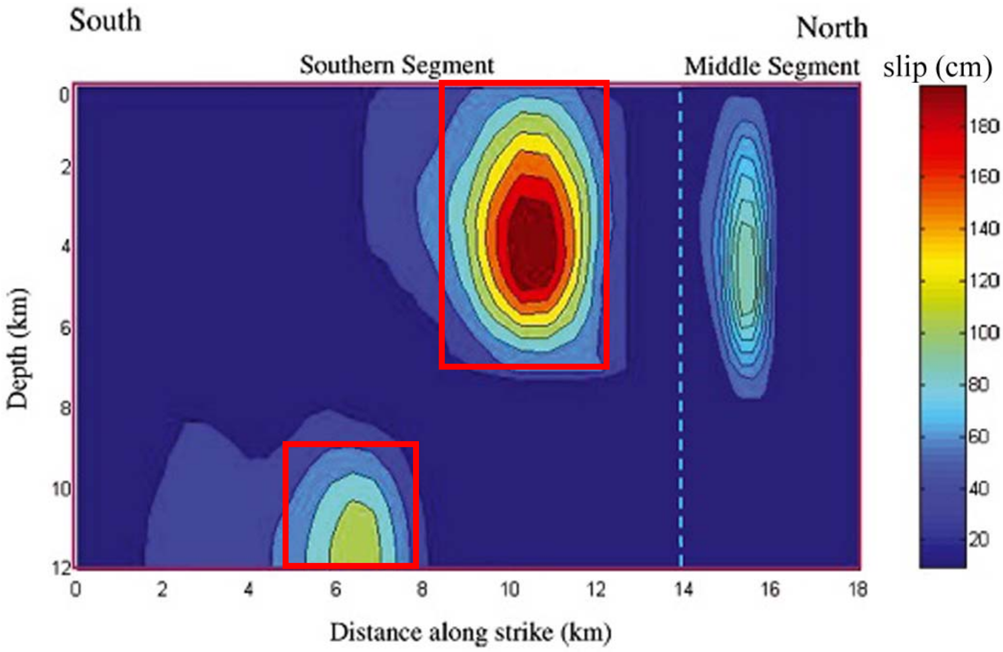

Figure 4.1. Slip model of fault plane in Bam earthquake (Ghayamghamian and Hisada, 2007)

4.1. Dynamic source parameters of Bam fault

Based on Somerville et al. (2000) definition, an asperity contains sub-faults whose slip is 1.5 or more times larger than the average slip over the fault. Thus, the sub-faults with the slip larger than 50 cm are assumed to be the asperity regions as shown by red rectangular in Fig. 4.1.

Based on explanation given by Tinti et al. (2009) and Mikumo et al. (2003), we assumed the ratio of D_c/D_{tot} to be 0.45. Then, the slip-weakening distance in main asperity of Bam fault evaluated to be in the range of 20 to 55 cm. Based on Eqn. 2.3, the static stress drop can be found after estimating the shear modulus from Eqn. 2.4. The shear modulus calculated using provided density in structural model by Ghayamghamian and Hisada (2007) as shown in table 4.1. It is noteworthy that the slip was occurred in two layers. Consequently, the static stress drop and its distribution on the fault are calculated as shown in Fig. 4.2. The ratio of background stress drop to average asperity stress drop is founded to be 39%, which is in agreement with the theoretical asperity model of Das and Kostrov (1986). According to Das and Kostrov criteria, average stress drop of an asperity (with radius r) is increased by the ratio (R/r) over the average stress drop on the surrounding annular crack area (with radius R) (Das and Kostrov 1986). Finally, using Eqn. 2.5, dynamic stress drop throughout the fault plane is calculated. The identified dynamic source parameters for two asperities of Bam fault are summarized in table 4.2.

Table 4.1. Fault zones with various shear wave velocity

Fault zones	Depth (km)	V_s (m/s)	μ (Mpa)
Layer 1	0-8	3550	35000
Layer 2	8-12	3800	40000

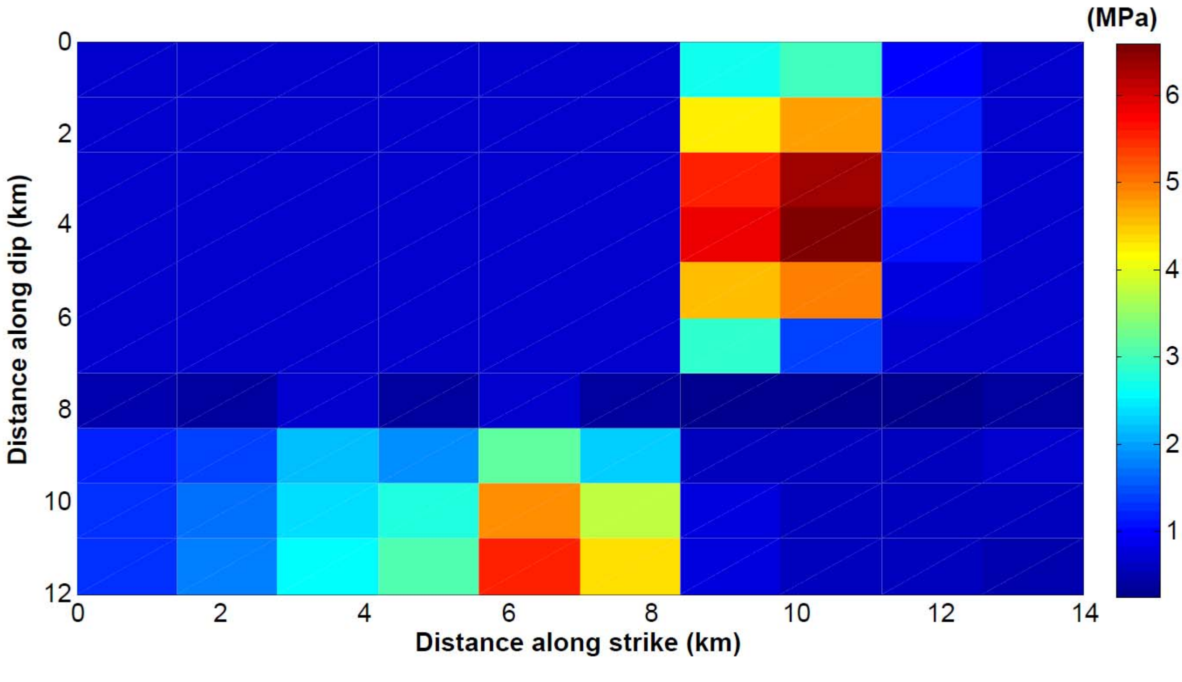

Figure 4.2. Distribution of static stress drop on fault plane

Table 4.2. Dynamic source parameters for two asperities of Bam fault

Area of asperity (km^2)	18.48	6.72
Slip weakening distance (cm)	22-55	28-35
Static stress drop (bar)	16-66	38-60
Dynamic stress drop (bar)	26-63	36-53
Strength excess (bar)	43-100	57-86

5. ENERGY BALANCE ON THE BAM FAULT

Based on Eqn. 3.3, the spatial distribution of near-source energy is estimated as illustrated in Fig. 5.1. As shown in this figure, the maximum near-source energy released from main asperity with the value of 3.2 MJ/m^2. Furthermore, the distribution of fracture energy is estimated and shown in Fig. 5.2. The parameters of near-source energy released for the two asperities are summarized in table 5.1. Another parameter involved with released energy of an earthquake is radiation efficiency, which can be calculated as:

$$\eta_R = \frac{E_r}{E_r + E_F} \tag{5.4}$$

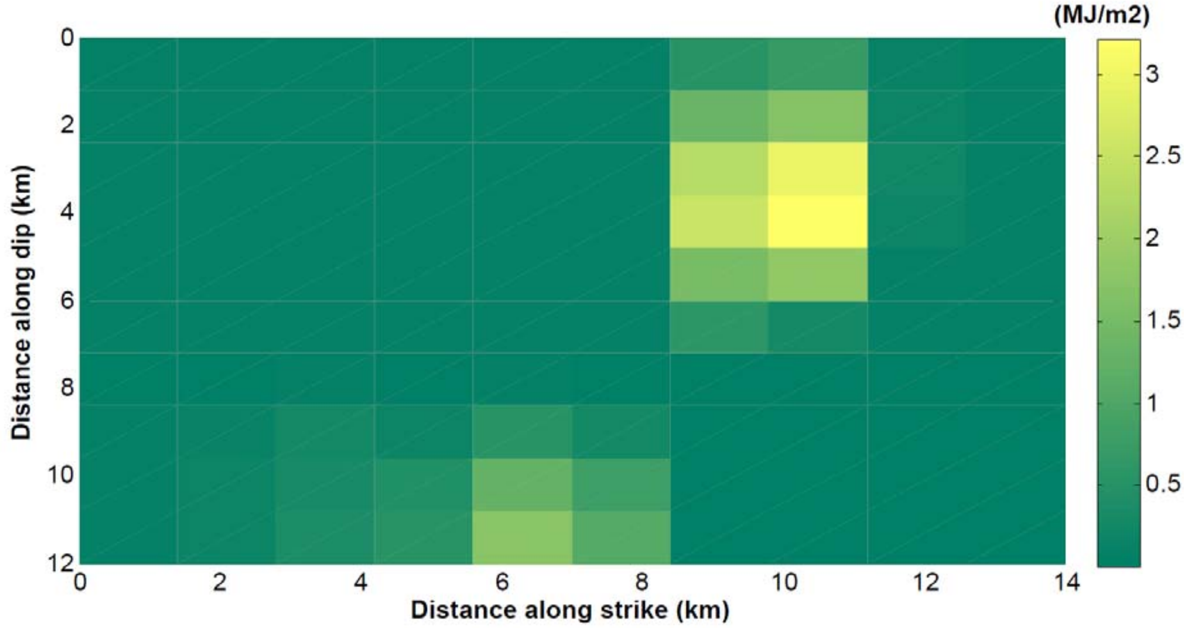

Figure 5.1. Spatial distribution of near-source energy of Bam fault

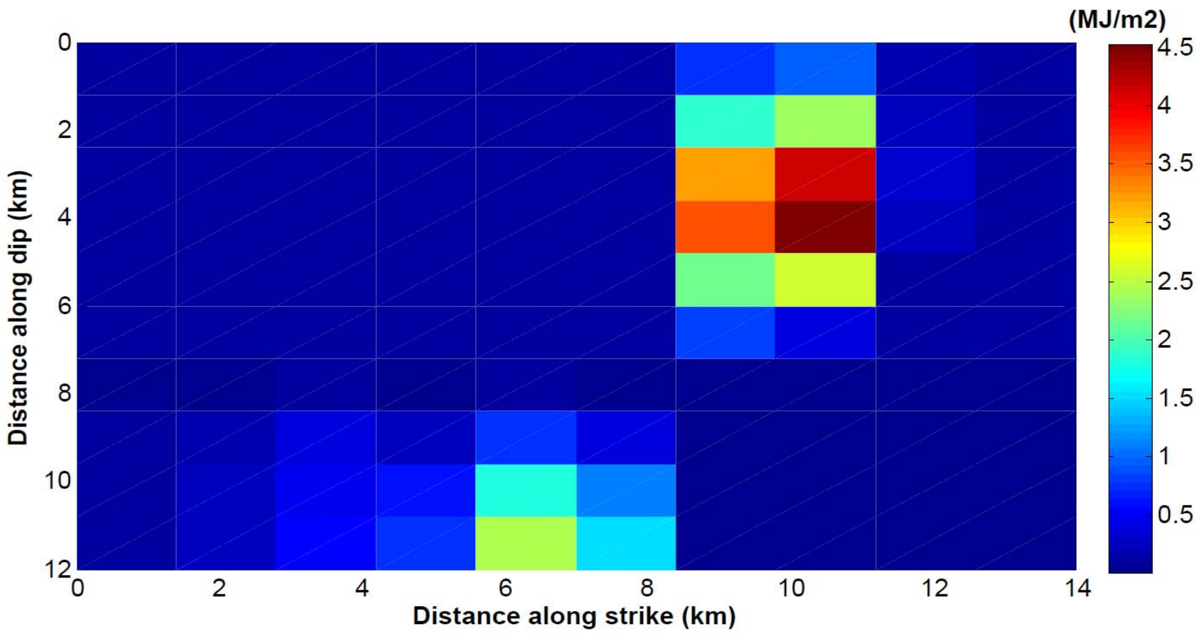

Figure 5.2. Distribution of fracture energy on fault plane in Bam earthquake

Table 5.1. Energy released parameters for asperities of Bam fault

Dimension of fault	14 km × 12 km	
Area of asperity (km^2)	18.48	6.72
$\frac{E_F}{A}$ (MJ/m2)	0.7-4.53	1.1-2.4
$\frac{E'_r}{A}$ (MJ/m2)	0.6-3.2	0.8-1.7
E_F (10^7MJ)	4.5	1.2
E'_r (10^7MJ)	3.2	0.8
$\frac{E'_r}{E_F}$	0.71	0.71

where η_R is radiation efficiency. Venkataraman and Kanamori (2004) estimated radiation efficiency for several crustal earthquakes and showed that this parameter for most earthquakes lies in the range of 0.25 to 1. However, Tsunami earthquakes have smaller radiation efficiencies than 0.25 (Venkataraman and Kanamori, 2004). The radiation efficiency for Bam fault is founded to be 0.42, which is in accordance with other crustal earthquakes.

6. CONCLOUSION

In this study, dynamic source parameters together with the near-source and fracture energies of Bam fault were estimated using Fukuyama's new energy balance relation and linear slip-weakening model (Fukuyama 2005). The maximum Slip-weakening distance, static and dynamic stress drop and strength excess were revealed to be 55 cm, 66 bar, 63 bar and 100 bar respectively.
Near-source released energy and fracture energy of bam fault asperities were found to be in the range of 0.6 to 3.2 MJ/m^2 and 0.7 to 4.53 MJ/m^2, respectively. The near-source energy released from the major asperity of Bam earthquake is lower than fracture energy. This might be in accordance with the assumption of new fault rupture scenario for the Bam earthquake (Ye 2005; Fu, et al. 2007; Ghayamghamian and Hisada 2007). Thus, most of potential energy was dissipated as fracture energy for creating new fault. The radiation efficiency was estimated to be 0.42, which is in agreement with the values founded for Hector earthquake (1999) and Izmit earthquake (1999) by Venkataraman and Kanamori (2004).

REFERENCES

Andrews, D. J. (1976). Rupture velocity of plane strain shear cracks. *Journal of Geophysical Research*. **81,** 5679-5687.

Chester, J.S., F.M. Chester, and A.K. Kronenberg (2005). Fracture surface energy of the Punchbowl fault, San Andreas system, *Nature*. **437**, 133-136.

Das, S., and Kostrov, B. V. (1986). Earthquake Source Mechanics. AGU.

Fu, B., Lei, X., Hessami, K., Ninomiya, Y., Azuma, T., and Kondo, H. (2007). A new fault rupture scenario for the 2003 Mw 6.6 Bam earthquake, SE Iran: Insights from the high-resolution QuickBird imagery and field observations. *Journal of Geodynamics*. **44 :3-5**, 160-172.

Fukuyama, E. (2005). Radiation energy measured at eartthquake source. *Geophysical research letters*. **32: L13308**

Fukuyama, E., Mikumo, T., and Olsen, K. B. (2003). Estimation of the Critical Slip-Weakening Distance: Theoretical Background. *Bulletin of the Seismological Society of America*. **93: 4**, 1835–1840.

Funning, G.J., Parsons, B., Wright, T.J., Jackson, J.A. & Fieding, E.J., 2005. Surface displacement and source parameters of the 2003 Bam (Iran) earthquake from Envisat advanced synthetic aperture radar imagery, *J. Geophy. Res.,* **110: B09406**, doi: 10.1029/2004JB003338.

Ghayamghamian, M. R., and Hisada, Y. (2007). Near-fault strong motion complexity of the 2003 Bam earthquake (Iran) and low-frequency ground motion simulation. *Geophys. J. Int*. **170**, 679-686.

Ida, Y. (1972), Cohesive force across the tip of a longitudinal‒shear crack and Griffith's specific surface energy, *J. Geophys. Res.* **77**, 3796-3805.

Rouhollahi, R., Ghayamghamian M. R., Yaminifard F., Suhadolc P., Tatar M. (2012). Source process and slip model of 2005 Dahuiyeh-Zarand earthquake (Iran) using inversion of near-field strong motion data. *Geophys. J. Int.***189:1,** 669-680

Knopoff, L. (1958). Energy release in earthquakes. *Journal of Geophys*. 44–52.

Mai, P. M., Somerville, P., Pitarka, A., Dalguer, L., Song, S., Beroza, G., et al. (2006). On Scaling of Fracture Energy and Stress Drop in Dynamic Rupture Models: Consequences for Near-Source Ground-Motions. *Earthquake: Radiated Energy and the Physics of Faulting, Geophysical Monograph*. **170**.

Mikumo, T., and Fukuyama, E. (2006). Near source released energy in relation to fracture energy on earthquake faults. *Bulliten of the seismological society of america.* **96: 3**, 1177-1181 .

Mikumo, T., Olsen, K. B., Fukuyama, E., and Yagi, Y. (2003). Stress-Breakdown Time and Slip-Weakening Distance Inferred from Slip-Velocity Functions on Earthquake Faults. *Bulletin of the Seismological Society of America*. **93: 1**, 264–282.

Nakamura, T. et al., 2005. Source fault structure of the 2003 Bam earthquake, southeastern Iran, inferred from the aftershock distribution and its relation to the heavily damaged area: existance of the Arg-e-Bam fault proposed, *Geophysical research letters.* **32: L09308**, doi: 10.1029/2005GL022631.

Rice, J.R., Sammis, C.G. and Parsons, R. (2005), Off-fault secondary failure induced by a dynamic slip pulse, *Bull Seismol. Soc. Am.*, **95**, 109-134.

Rivera, L., and Kanamori, H. (2005). Representations of the radiated energy in earthquakes. *Geophys. J. Int. ,* **162**, 148–155.

Scholz, C. H. (1998). Earthquakes and friction laws. *nature*. **391**.

Senatorski, P. (2002). Slip-weakening and interactive dynamics of an heterogeneous seismic source. *Tectonophysics*. 37-60.

Somerville, P. G., Irikura, K., Abrahamson, N., Sawada, S., Kagawa, T., and Tatsumi, Y. (2000). characterizing earthquake slip models for the prediction of strong ground motion. *12th World Conferences on Earthquake engineering.*

Talebian, M. et al. *(*2004). The 2003 Bam (Iran) earthquake: rupture of a blind strike-slip fault, *GRL,* **31,** L11611, doi: 10.1029/2004GL020058.

Tinti, E., Cocco, M., Fukuyama, E., and Piatanesi, A. (2009). Dependence of slip weakening distance (Dc) on final slip during dynamic rupture of earthquakes. *Geophys. J. Int.* **177,** 1205–1220.

Tinti, E., Spudich, P., and Cocco, M. (2005). Earthquake fracture energy inferred from kinematic rupture models on extended faults. *journal of geophysical research.* **110**: **B12303**.

Venkataraman, A., and Kanamori, H. (2004). Observational constraints on the fracture energy of subduction zone earthquakes. *journal of geophysical research*. **109:B05302.**

Wang, R., Xia, Y., Grosser, H., Wetzel, H.U., Kaufmann, H. & Zschau, J., (2004). The 2003 Bam (SE Iran) earthquake: precise source parameters from satellite radar interfrometry, *Geophys. J. Int.,* **159,** 917–922.

Wibberley, C. A., and Shimamoto, T. (2005). Earthquake slip weakening and asperities explained by thermal pressurization. *nature.* **436.**

Wilson, B., Dewers T., Reches, Z. and Brune, J. (2005), Particle size and energetics of gouge from earthquake rupture zonessss, *Nature,* **434**, 749-752.

Xing, H. L., Mora, P., et al. (2006). A unified friction description and its application to the simulation of frictional instability using the finite element method. *Philosophical Magazine*. **86**, 3453–3475.

Ye, X. (2005). Bam earthquake: Surface deformation measurement using radar interferometry. *acta seismologica sinica*. **18:4**, 451-459.